

# DESIGN STUDY AND MODELING OF THE RF SECTION FOR AN S-BAND HIGH-EFFICIENCY MULTI-BEAM KLYSTRON

S. Wang<sup>†</sup>, S. Matsumoto, T. Natsui, T. Matsumoto, T. Miura, S. Fukuda, KEK, Tsukuba, Ibaraki 305-0801, Japan

## Abstract

An S-band high-efficiency multi-beam klystron is currently in development to modernize the existing 50MW klystron utilized in the KEK  $e^-/e^+$  Injector Linac. The RF section and collector design are introduced in this paper. Initial parameter selection for the RF section is facilitated using a two-dimensional particle-in-cell code. The final design comprises 6 cavities, projecting an efficiency of 76%. Subsequently, A detailed three-dimensional model and particle-in-cell simulation confirm the efficiency of 72.5%. Tolerance analysis is performed to assess practical scenarios deviating slightly from the design specifications. The impact of a high-order mode on klystron performance is analyzed through three-dimensional simulation. Lastly, in the collector, the maximum heat flux under the condition of the full-power beam and the particles' motion of the spent beam are presented.

## INTRODUCTION

The KEK  $e^-/e^+$  Injector Linac adopts 60 pulsed 50 MW S-band klystrons [1] with an efficiency of 45%. A multi-beam klystron (MBK) with an efficiency of 70% and an output power of 80 MW is under development for replacement, primarily for two purposes. First, if the klystron efficiency could be improved from 45% to 70%, a total energy of 2640 MWh would be saved over an entire year of operation. Second, with the output power increased from 50 MW to 80 MW, the RF power margin of the KEK  $e^-/e^+$  Injector Linac would be significantly improved.

As a worldwide concern, large-scale accelerators increasingly demand high-efficiency klystrons to reduce massive operating costs. The KEK 80 MW MBK, named KMS80, aims to achieve dual records in both efficiency and output power for S-band MBKs. This paper introduces the design of the RF section and collector for the KMS80.

## RF SECTION

### Overall Parameters

For the design of a high-efficiency klystron, the overall parameter design must necessarily minimize the beam perveance [2]. However, a lower beam perveance generally leads to a higher gun voltage, which can negatively affect the operational stability of the klystron. The MBK has a natural advantage in that it can achieve extremely low perveance while maintaining the electron gun voltage within a reasonable range. The ring-shaped cavity, which operates on its fundamental  $TM_{010}$  mode, is chosen due to

its advantageous combination of high R/Q and flexible arrangement of multiple beamlets. Figure 1 shows the configuration and longitude E-field distribution of the  $TM_{010}$  mode in an S-band ring-shaped cavity with 8 beamlets. Table 1 lists the overall parameters relating to the RF section.

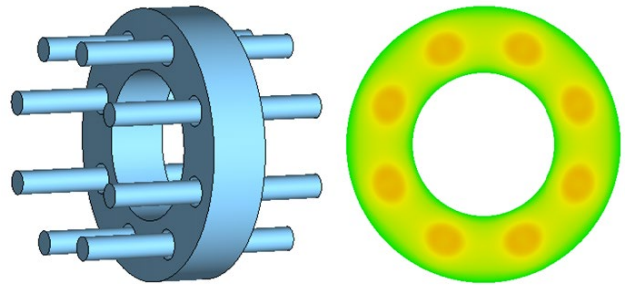


Figure 1: The configuration of the ring-shaped cavity and its longitude E-field distribution of the fundamental mode.

Table 1: Overall Parameters Relating to the RF Section

Parameter	Value
Frequency	2856 MHz
Beam voltage	300 kV
Beam current	45.8 A * 8
Beam perveance	0.28 $\mu\text{A}/\text{V}^{3/2}$
Beam tunnel radius	7.5 mm
Beamlets distribution radius	65 mm

The individual beam perveance is as low as 0.28  $\mu\text{A}/\text{V}^{3/2}$ , representing a low space charge force level. The beam tunnel radius of 7.5 mm guarantees a cut-off frequency four times higher than the operating frequency. This allows the use of harmonic cavities for bunching. The distance from the center of the beam tunnel to the center of the cavity is 65 mm. This dimension leaves enough space for individual collectors rather than a shared collector, preventing reflected electrons from easily returning to the RF section [3].

### Two-dimensional Simulation

We skip the one-dimensional simulation, commonly considered fast but lacking in accuracy. Instead, we combine the two-dimensional EMSYS software [4] and a genetic algorithm [5] as a tool for automatically optimizing the cavity layout parameters. EMSYS is a fast quasi-PIC software suitable for the massive simulations required by the genetic algorithm.

For the first step, we chose a cavity layout, where the number and type of cavities (fundamental or harmonics) are decided. Secondly, the parameters of the layout, includ-

<sup>†</sup> shengchang.wang@kek.jp

ing frequencies, distances, etc., are automatically optimized with the criteria of higher efficiency and a shorter layout. For the third step, the result from the automatic optimization is manually checked, and a new layout is decided, returning to the first step. After several iterations, the final choice is made based on the standards of high efficiency, short layout length, and fewer cavities. Figure 2 shows the chosen layout. The beam is divided into five layers based on radius. The phase diagrams of the five-layer beams differ, showing that the beam at the lower radius endures weaker modulation. This is called the radial stratification effect due to the E field non-uniformity inside the gap region of a cavity.

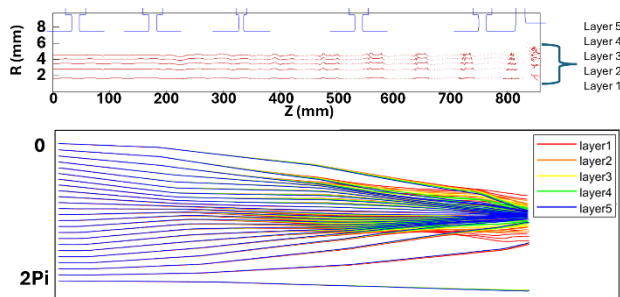


Figure 2: The chosen layout and phase diagrams with a radial stratification effect.

The EMSYS simulation predicts an efficiency of 76%, with a total of six cavities, including one 2nd harmonic cavity. The transfer curve and bandwidth curve from EMSYS are shown in Fig. 3.

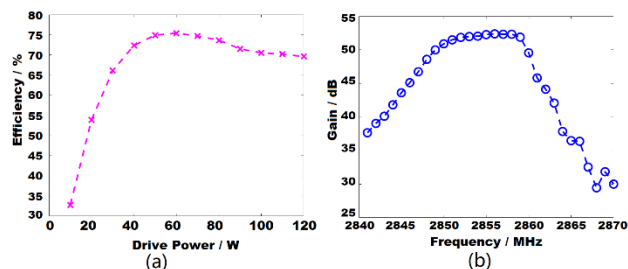


Figure 3: The transfer curve (a) and bandwidth curve (b) from EMSYS.

### Three-dimensional Simulation

The three-dimensional PIC software CST [6] is employed to perform a confirmation to the two-dimensional result. Figure 4(a) shows the model and a snapshot of particle motion in the MBK. The output cavity adopts two waveguide ports to achieve a uniform field distribution among the beamlets. Additionally, two waveguides facilitate the use of two RF windows, resulting in an RF power of 40 MW per window. As the existing RF window cannot handle an RF power of 80 MW, the design with two RF windows will be more reliable.

The output signal from one of the ports is shown in Fig. 4(b), and the wave-particle power transfer curve is shown in Fig. 4(c). The output power can be calculated both from the square of the rms value of the output signal and the mean of the wave-particle power transfer curve.

Due to the use of dispersion to reduce numerical noise [7], the values from the two approaches differ slightly, within 0.8%, which is considered acceptable. The consequently calculated efficiency is 73.3%. Considering the RF circuit efficiency of 99%, the overall efficiency is 72.5%. Figure 4(d) shows the frequency spectrum of the output signal, with the largest component located at the fundamental frequency of 2856 MHz, and smaller, gradually decreasing components at higher order harmonics.

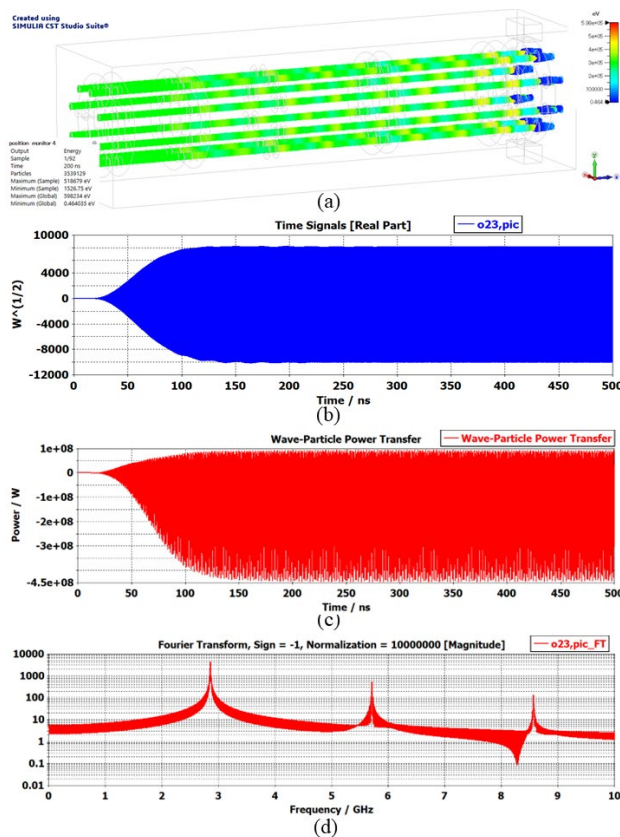


Figure 4: (a) The 3-D model and a snapshot of particle motion, (b) The output signal from one of the waveguide ports, (c) The wave-particle power transfer curve, (d) The frequency spectrum of the output signal.

### Tolerance Analysis

Tolerance analysis evaluates practical scenarios that slightly deviate from the designed values or conditions. In real situations involving the electron gun and focusing magnetic field, there might be slight beam off-center issues or errors in the beam filling factor. CST is used to evaluate these real situations while maintaining a fixed drive power. The efficiency distribution with the variation of the beam filling factor and beam off-center is shown in Fig. 5. The horizontal axis represents the beam filling factor, while the vertical axis indicates the beam off-center value. Figure 5 demonstrates that there is a region where the efficiency remains higher than 70%. The beam filling factor seems to have a greater influence on the efficiency, which is not surprising since differences in the beam filling factor affect the extent of cavity-beam coupling. If the beam filling factor is less than the designed value, increasing the drive

power (thereby decreasing the gain) can recover some efficiency. Similarly, if the beam filling factor is greater than expected, decreasing the drive power (thereby increasing the gain) can also recover some efficiency.

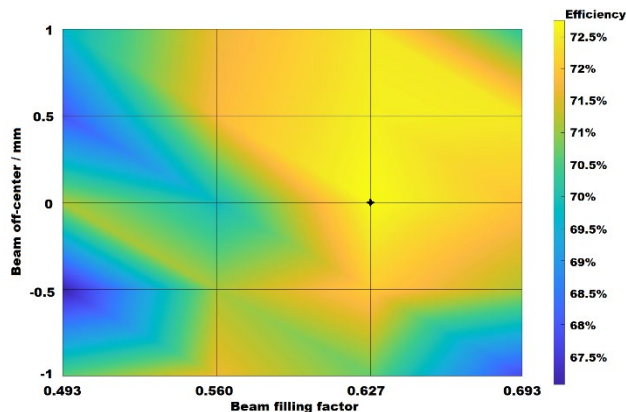


Figure 5: The efficiency distribution with the variation of beam filling factor and beam off-center.

In practice, the cavities are not always tuned to the exact design values. Therefore, a tuning error range is defined for each cavity. The EMSYS software is used to investigate cases with random frequency errors within this range. Figure 6 shows a statistical analysis of these random cases. For most scenarios, the efficiency remains higher than 72%. Since the drive power is fixed for all these cases, it is investigated and found that for cases with efficiency lower than expected, adjusting the drive power could recover part of the efficiency.

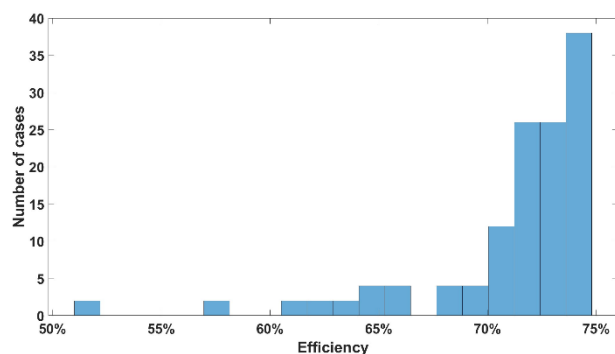


Figure 6: The efficiency statistic with random errors for cavity frequencies.

### High order Modes

CST can predict potential instabilities arising from high-order modes in beam-wave interaction simulations. For example, our simulation revealed that the 2nd harmonic ring-shaped cavity operates in a mixed state of  $TM_{010}$  mode and  $TM_{110}$  mode. The presence of  $TM_{110}$  differs the longitudinal beam motion in different beamlets. Consequently, individual pillbox cavities are used instead of a ring-shaped 2nd harmonic cavity. Figure 7 shows the change in mode pattern over half an RF period inside the ring-shaped 2nd harmonic cavity, monitored during a PIC simulation with CST.

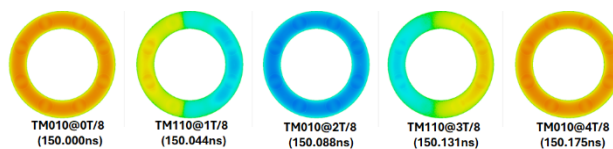


Figure 7: The altering of  $TM_{010}$  and  $TM_{110}$  modes over half an RF period inside the ring-shaped 2<sup>nd</sup> harmonic cavity.

## COLLECTOR

KMS80 adopts individual collectors. The length and inner radius of each collector are 230 mm and 14 mm, respectively, allowing for independent cooling channels. Under the full beam power, the maximum heat flux in the collector is  $210 \text{ W/cm}^2$ , a conservative value for water-cooled collector. With the focusing magnetic field imported [2], the collectors and the interaction region are incorporated together for a PIC simulation. As shown in Fig. 8, no back-electrons caused by space charge depression at the entrance region of the collector are observed.

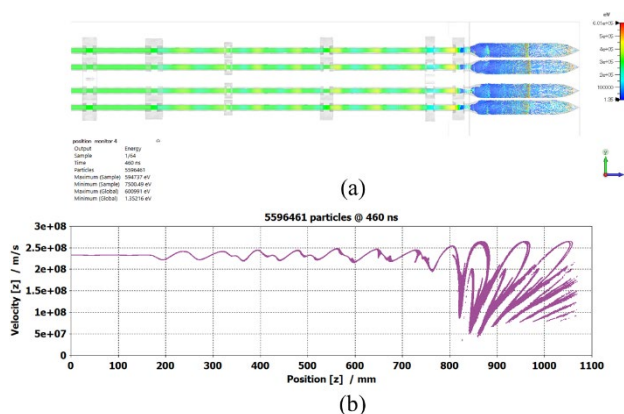


Figure 8: (a) A snapshot of particle motion in the interaction region together with the collectors, (b) The scatter plot of velocity versus longitude position for all the simulated particles at the same time.

## CONCLUSION

The RF section and collector are designed for the S-band MBK, which has an efficiency of 72.5% and an output power of 80 MW. The mechanical design is currently underway, with prototype building and testing expected in the coming year.

## REFERENCES

- [1] S. Fukuda *et al.*, “Design and evaluation of a compact 50 MW RF source of the PF linac for the KEKB project”, *Nucl. Instrum. Methods A*, vol. 368, pp. 561-571, 1996.
- [2] T. Natsui *et al.* “Design of the gun and the magnet for s-band 80 MW multi-beam pulsed klystron”, paper THP021, this conference
- [3] S. Wang *et al.*, “Design study and modeling of multi-beam Klystron for Circular Electron Positron Collider”, *Nucl. Instrum. Methods A*, vol. 1026, 166208, 2022.
- [4] T. Shintake, “Klystron simulation and design using the Field Charge Interaction (FCI) code”, *Nucl. Instrum. Methods A*, vol. 363, pp. 83-89, 1995.

- [5] A. Seshadri, "A fast elitist multiobjective genetic algorithm: NSGA-II", *MATLAB Central*, vol. 182, pp. 182-197, 2006.
- [6] CST Studio Suite, <https://www.3ds.com/products/simulia/cst-studio-suite>
- [7] S. A. Kurkin *et al.*, "Modeling instabilities in relativistic electronic beams in the CST Particle Studio Environment", *Math Models Comput Simul*, vol. 10, pp. 59-68, 2018.